

What Powers the $12\ \mu\text{m}$ Luminosities in AGNs: Spitzer/IRS Spectroscopic Study of the $12\ \mu\text{m}$ Seyfert Sample

Yanling Wu

*Infrared Processing and Analysis Center, California Institute of
Technology, MC 314-6, 1200 East California Blvd, Pasadena, CA,
91125*

Jiasheng Huang

*Harvard-Smithsonian Center for Astrophysics, 60 Garden Street,
Cambridge, MA, 02138*

Vassilis Charmandaris

*University of Crete, Department of Physics, GR-71003, Heraklion,
Greece*

*IESL/Foundation for Research and Technology - Hellas, GR-71110,
Heraklion, Greece, and Chercheur Associé, Observatoire de Paris,
F-75014, Paris, France*

Abstract. We present a mid-IR study of the $12\ \mu\text{m}$ Seyfert sample, using $5\text{-}35\ \mu\text{m}$ low-resolution spectroscopy from Spitzer/IRS. Sources in this sample display a wide variety of spectral shapes. We perform an analysis of the continuum emission, the strength of the Polycyclic Aromatic Hydrocarbon (PAH) emission, as well as fine-structure lines, in order to study the mid-IR properties of the local Seyfert galaxies. We find that the equivalent widths of PAHs decrease with increasing dust temperature. We also propose a method to estimate the AGN contribution to the integrated $12\ \mu\text{m}$ emission of the galaxy.

1. Introduction

Active Galactic Nuclei (AGNs) are compact regions in galaxies, which have higher than normal luminosities, produced by non-stellar activities, such as accretion onto the super-massive black hole located at the center of galaxies. As a subclass of AGNs, Seyfert galaxies have 2-10 keV X-ray luminosities less than $\sim 10^{44}\ \text{ergs}^{-1}$, and spectral line emission from highly ionized gas. Optical spectroscopic studies of Seyferts have led to the classification of two types, Seyfert 1s (Sy 1s), which display both broad ($\text{FWHM} > 2000\ \text{km s}^{-1}$) and narrow emission lines, and Seyfert 2s (Sy 2s), which only display narrow-line emission.

Seyfert galaxies have been observed at many wavelengths, from X-ray, ultraviolet, optical, to infrared and radio. The mid-infrared (mid-IR) spectroscopy is a powerful tool to examine the nature of the emission from AGNs, as well as the associated star-formation activities. Because infrared observations are much less affected by dust extinction, they have been instrumental in the study

of obscured emission from optically thick regions in AGNs. This is crucial for understanding the physical process of galaxy evolution.

The extended $12\ \mu\text{m}$ galaxy sample is a flux-limited ($0.22\ \text{Jy}$ at $12\ \mu\text{m}$) sample of 893 galaxies selected from the IRAS Faint Source Catalog 2 (Rush et al. 1993). Selecting active galaxies based on their rest frame $12\ \mu\text{m}$ fluxes is the best approach to reduce selection bias due to the variations in their intrinsic spectral energy distributions (SEDs), because all galaxies emit a nearly constant fraction of their bolometric luminosities at $12\ \mu\text{m}$ (Spinoglio & Malkan 1989). A total of 116 objects from this sample have been classified optically as Seyfert galaxies (53 Sy 1s and 63 Sy 2s), providing one of the largest IR selected unbiased sample of AGNs. In this paper, we study the nature of the nuclear dust enshrouded emission from AGNs, using 5-35 μm low-resolution spectroscopy from Spitzer/IRS.

2. Data Reduction

A large fraction of the $12\ \mu\text{m}$ Seyfert galaxies have been observed by various programs using Spitzer/IRS and data are publicly available. We retrieved low-resolution data for 103 galaxies from the Spitzer archive. For observations taken by the IRS mapping mode, we used The CUbe Building for IRS Spectra Maps (CUBISM, Smith et al. 2007a) to build spectral cubes. Then we extracted the spectra using matched apertures of varying size, chosen to encompass the nuclear, as well as useful regions of the disk. For data taken in the IRS staring mode, the reduction started from the intermediate pipeline products droop files. After median combination and background subtraction, the 2-D images were extracted with the Spectral Modelling, Analysis, and Reduction Tool (SMART, Higdon et al. 2004) using a variable width aperture, which scales with wavelength to recover the same fraction of the diffraction limited instrumental point-spread-function.

3. Results

3.1. Global Mid-IR Spectra of Seyfert Galaxies

The mid-IR spectra of Seyfert galaxies display a variety of features (see Clavel et al. 2000; Verma et al. 2005; Weedman et al. 2005; Buchanan et al. 2006; Hao et al. 2007, and references therein). Our complete $12\ \mu\text{m}$ selected Seyfert sample provides an unbiased framework to study the statistics on their mid-IR properties. In the left panel of Figure 1., we display the average spectra of Sy 1s (solid line) and Sy 2s (dotted line) with full 5.5-35 μm spectral coverage. For comparison, we also overplot the average starburst template from Brandl et al. (2006). It is clear that the mid-IR continuum slope of the average Sy 1 spectrum is much shallower than that of the average Sy 2, while the starburst template has the steepest spectral slope, indicating a different mixture of hot/cold dust component in these galaxies. PAH emission, which is a good tracer of star formation activity, can be detected in the average spectra of both Seyfert types, while it is strongest in the average starburst spectrum. High ionization fine-structure lines, such as [NeV] $14.32\ \mu/24.32\ \mu\text{m}$, which serve as unbiased indicator of AGN, are

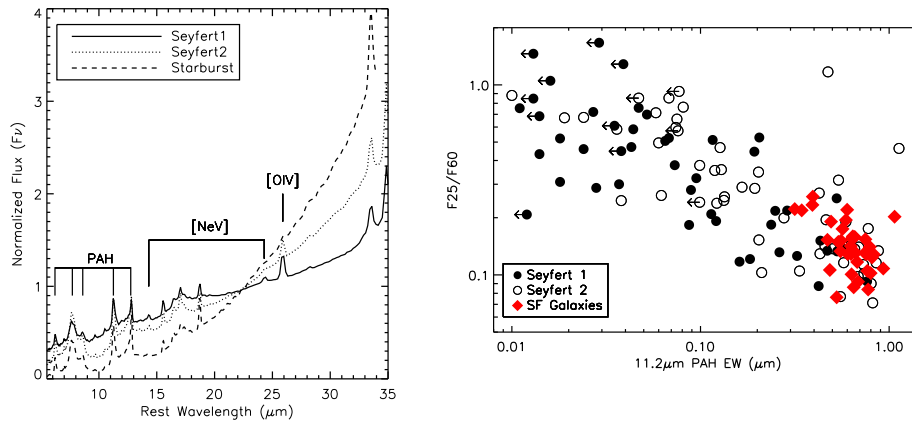


Figure 1. Left panel: A comparison among the average mid-IR spectrum of Sy 1s (solid line) and Sy 2s (dotted line) of the 12 μm sample, as well as the starbursts (dashed line) of Brandl et al. (2006). All spectra have been normalized at 22 μm . Right panel: The IRAS 25 to 60 μm flux ratio (F_{25}/F_{60}) as a function of the 11.2 μm PAH EW for the 12 μm Seyfert sample. The filled circles are Sy 1s, and the open circles are Sy 2s. The diamonds represent the SF galaxies from Brandl et al. (2006) and Smith et al. (2007b).

clearly detected even in the low-resolution average spectrum of Sy 1. This signature is also visible, though rather weak, in the average Sy 2 spectrum, while it is absent in the average starburst template. Another high ionization line, [OIV] 25.89 μm , also appear in both Seyfert types, and is stronger in the average Sy 1 spectrum. The [OIV] emission line can be powered by shocks in intense star forming regions or AGNs (see Lutz et al. 1998; Bernard-Salas et al. 2009; Hao et al. 2009), and in our sample, it is probably powered by both, given the size of the aperture we adopted for spectral extraction.

3.2. What Powers the 12 μm Luminosities of Seyferts?

The use of the global infrared dust emission as a tracer of the absorbed starlight and associated star formation rate has been known since the first result of IRAS (Kennicutt 1998). In the left panel of Figure 2, we plot the 12 μm luminosity versus the total IR luminosity for the Seyfert galaxies. For comparison, we have also included the starburst galaxies from Brandl et al. (2006) and HII galaxies from Smith et al. (2007b). A clear correlation between the two parameters is seen. The two Seyfert types do not show significant difference, while we notice that they appear to be located higher than the star forming galaxies on this plot. This can be explained by the presence of additional hot dust emission originating from regions near the active nucleus, and it is consistent with the results of Spinoglio et al. (1995), who reported that the 12 μm luminosity is $\sim 15\%$ of the total IR luminosity for AGNs, while only $\sim 7\%$ in starburst and normal galaxies.

To better understand the role of an AGN, we seek to distinguish the AGN from star formation signatures in the mid-IR to determine its fractional contribution. In the middle panel of Figure 2, we plot the 11.2 μm PAH lumi-

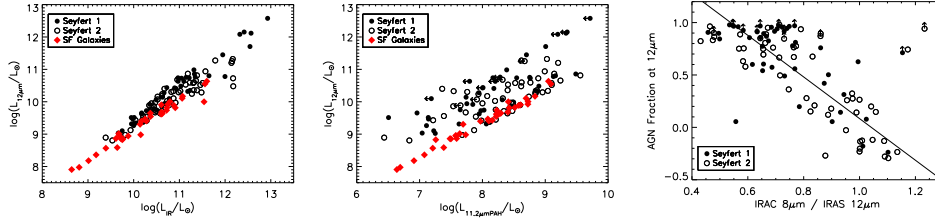


Figure 2. Left panel: The $12\ \mu\text{m}$ luminosity versus the total infrared luminosity of the $12\ \mu\text{m}$ Seyfert sample. The Seyfert 1s are represented with filled circles, while Seyfert 2s are indicated with open circles and star-forming galaxies with diamonds. Middle panel: The $12\ \mu\text{m}$ luminosity versus the $11.2\ \mu\text{m}$ PAH luminosity of the $12\ \mu\text{m}$ Seyfert sample. Right panel: The AGN fraction at $12\ \mu\text{m}$ as a function of the IRAC $8\ \mu\text{m}$ to *IRAS* $12\ \mu\text{m}$ flux ratio. The solid line is a fit to the Seyfert galaxies excluding those with lower limits for the AGN fraction.

nosity versus the $12\ \mu\text{m}$ luminosity for the Seyferts and star-forming galaxies. There is a very tight correlation for SF galaxies with an average $L(11.2\ \mu\text{m PAH})/L(12\ \mu\text{m})=0.044\pm 0.010$. Since there is no AGN contamination in these galaxies, we attribute all of that to star formation. Seyfert galaxies display a large scatter on this plot, and we decompose its $12\ \mu\text{m}$ luminosity into two parts: one contributed by star-formation, and one contributed by AGN. We estimate the star formation contribution to the $12\ \mu\text{m}$ luminosity of Seyferts using the same correlation existing in SF galaxies. Subtracting the SF contribution from the $12\ \mu\text{m}$ luminosity, we can obtain, in a statistical sense, the corresponding AGN contribution.

To check the validity of this method, we plot in the right panel of Figure 2 the “AGN fraction” as a function of the IRAC $8\ \mu\text{m}$ to *IRAS* $12\ \mu\text{m}$ flux ratio. The IRAC $8\ \mu\text{m}$ flux will be dominated by PAH emission when PAHs are present, thus normalizing by the $12\ \mu\text{m}$ continuum provides an estimate of the equivalent width (EW) of PAHs. On the plot, we can see an anti-correlation between the two parameters, thus suggesting that our method of decomposing the $12\ \mu\text{m}$ luminosity is reasonable. This can be further applied to the study of distant universe, where spectroscopy becomes much more difficult, while using broad-band colors, one can estimate the “AGN fraction” of those galaxies.

3.3. Cold/Warm AGN Diagnostics

The *IRAS* 25 and $60\ \mu\text{m}$ flux ratio has been long used to determine the infrared color of a galaxy with “warm” galaxies having a ratio of $F_{25}/F_{60} > 0.2$ (Sanders et al. 1988). In the right panel of Figure 1, we display the $11.2\ \mu\text{m}$ PAH EW versus the galaxy color. We can see a clear trend of PAH EW decreasing with F_{25}/F_{60} . All SF galaxies appear to be clustered at the right bottom corner of the plot, having high PAH EW and low F_{25}/F_{60} ratio, suggesting strong star formation and cooler dust temperature. The observed suppression of PAH emission seen in the warm sources implies that the soft X-ray and UV radiation of the accretion disk, which destroys the PAH molecules, is also reprocessed by the dust and dominates the mid- and far-IR colors.

4. Summary

We have analysed Spitzer/IRS data for a complete IR selected unbiased sample of Seyfert galaxies. The main results of this study are:

1. The $12\mu\text{m}$ Seyferts display a wide variety of mid-IR spectral features. The continuum slope of Sy 1s appear to be shallower than Sy 2s. PAH emission is detected in both types, and AGN signature, as indicated by the [NeV] line emission, is stronger in Sy 1s than Sy 2s.

2. The $12\mu\text{m}$ luminosity of Seyfert galaxies can be decomposed to star-formation and AGN parts, using the existing correlation between PAH and mid-IR luminosity of SF galaxies. This can be further applied to the study of higher redshift galaxies.

3. The PAH EWs of Seyfert galaxies are more suppressed in warm AGNs, where the strong radiation field destroys the PAH molecules.

5. References

- Bernard-Salas, J., et al. 2009, ApJ Supplement, submitted
Brandl, B.R., et al. 2006, ApJ, 653, 1129
Buchanan, C.L., et al. 2006, AJ, 132, 401
Clavel, J., et al. 2000, A&A, 357, 839
Hao, L., et al. 2005, ApJ, 625, L75
Hao, L., et al. 2009, ApJ, submitted
Higdon, S.J.U., et al. 2004, PASP, 116, 975
Kennicutt, R.C. Jr. 1998, ARA&A, 36, 189
Lutz, D., et al. 1998, ApJ, 505, L103
Rush, B., et al. 1993, ApJS, 89,1
Sanders, D.B., et al. 19 1988, ApJ, 328, L35
Smith, J.D.T., et al. 2007a, PASP, 119, 1133
Smith, J.D.T., et al. 2007b, ApJ, 656 770
Spinoglio, L., & Malkan, M.A. 1989, ApJ, 342, 83
Spinoglio, L., et al. 1995, ApJ, 453, 616
Verma, A., et al. 2005, Space Sciences Reviews, 119, 335
Weedman, D.W., et al. 2005, ApJ, 633, 706



Yanling Wu



Yanling Wu, Junfeng Wang, and Hai Fu